Theoretical study of X− · 1·YF (1 = triazine, X = Cl, Br and I, Y = H, Cl, Br, I, PH2 and AsH2): Noncovalently electron-withdrawing effects on anion–arene interactions

ARTICLE *in* JOURNAL OF MOLECULAR MODELING · JANUARY 2014

Impact Factor: 1.74 · DOI: 10.1007/s00894-014-2076-0 · Source: PubMed

2 AUTHORS, INCLUDING:

Yishan Chen

Qujing Normal University

8 PUBLICATIONS **29** CITATIONS

SEE PROFILE

J Mol Model (2014) 20:2076
DOI 10.1007/s00894-014-2076-0

ORIGINAL PAPER

Theoretical study of $X^- \cdot 1 \cdot YF$ (1 = triazine, X = Cl, Br and I, Y = H, Cl, Br, I, PH_2 and AsH_2): noncovalently electron-withdrawing effects on anion-arene interactions

Yishan Chen · Lifeng Yao

Received: 24 September 2013 / Accepted: 12 November 2013 / Published online: 25 January 2014

Abstract The ternary complexes $X^- \cdot \mathbf{1} \cdot YF$ (**1** = triazine, X = Cl, Br and I, Y = H, Cl, Br, I, PH_2 and AsH_2) have been investigated by MP2 calculations to understand the noncovalently electron-withdrawing effects on anion-arene interactions. The results indicate that in binary complexes ($\mathbf{1} \cdot X^-$), both weak σ-type and anion-π complexes can be formed for Cl^- and Br^-, but only anion-π complex can be formed for I^-. Moreover, the hydrogen-bonding complex is the global minimum for all three halides in binary complexes. However, in ternary complexes, anion-π complex become unstable and only σ complex can retain in many cases for Cl^- and Br^-. Anion-π complex keeps stable only when YF = HF. In contrast with binary complexes, σ complex become the global minimum for Cl^- and Br^- in ternary complexes. These changes in binding mode and strength are consistent with the results of covalently electron-withdrawing effects. However, in contrast with the covalently electron-withdrawing substituents, Cl^- and Br^- can attack the aromatic carbon atom to form a strong σ complex when the noncovalently electron-withdrawing effect is induced by halogen bonding. The binding behavior for I^- is different from that for Cl^- and Br^- in two aspects. First, the anion-π complex for I^- can also keep stable when the noncovalent interaction is halogen bonding. Second, the anion-π complex for I^- is the global minimum when it can retain as a stable structure.

Keywords Anion-π interaction · Halogen bond · Hydrogen bond · Pnicogen bond · Supramolecular chemistry

Electronic supplementary material The online version of this article (doi:10.1007/s00894-014-2076-0) contains supplementary material, which is available to authorized users.

Y. Chen (✉) · L. Yao
School of Chemistry & Chemical Engineering, Qujing Normal University, Qujing 655011, Yunnan, China
e-mail: chenyishan916@163.com

Introduction

The various interactions of anions with arenes have attracted continuous interest from supramolecular and theoretical chemistry community due to their important role in anion recognition. As the experimental and theoretical studies have established, arenes, in particular electron-deficient arenes, can form a variety of complexes with anions [1–32]. When the halide anions lie above the plane of the π system, three different types of complex are possible: an anion-π complex, a strong σ-type complex and a weak σ-type complex. In addition, the aryl C-H · · · anion hydrogen-bonding complex is also common in supramolecular systems [8].

The covalently electron-withdrawing effects on anion-arene interactions have been extensively investigated and established [7]. Addition of electron-withdrawing substituents generally enhances all the anion-arene interactions mentioned above. When the halide anions lie above the aromatic ring, strongly nucleophilic F^- always leads to the strong σ complex with electron-deficient arene. Investigations on less nucleophilic halides, such as Cl^- and Br^-, have indicated that both weak σ and anion-π complexes can be formed with moderately electron-deficient arenes, such as triazine. However, as the electron affinity of the arene is increased, such as in tetracyanobenzene, the anion-π complex becomes unstable and only weak σ complex can remain. Moreover, when aryl C-H group is present, there is the possibility of competition between hydrogen bonding and π-system bonding for Cl^- and Br^- complexes. For moderately electron-deficient arenes, hydrogen-bonding interaction is stronger than weak σ and anion-π interactions. In contrast, weak σ interaction is stronger than hydrogen-bonding interaction for strongly electron-deficient arenes.

Since the covalently electron-withdrawing substituents have a great influence on the binding mode and strength of anion-arene systems, this leads us to ask, what about the noncovalently electron-withdrawing effect? The experimental

and theoretical studies of interplay between various noncovalent interactions have been reported in recent years [33–51]. Particularly, the Frontera and Lu groups have investigated the cooperative effects between anion-arene interactions and the other noncovalent interactions [33, 37, 51]. Although these studies are instructive and interesting, their investigations only concentrate on the anion-π interactions. A comprehensive study of noncovalently electron-withdrawing effects on the binding mode and strength of anion-arene syetems has not been reported up to now.

In this investigation, we select triazine (Fig. 1a, referred to as **1**) as a dual receptor molecule to understand the noncovalently electron-withdrawing effects on various anion-arene interactions. As a moderately electron-deficient arene, triazine can interact with halide anions (X^-) to form all four types of complexes mentioned above as shown in Fig. 1b-e: (1) anion-π interaction complexes, which can be formed with less nucleophilic halides (X = Cl, Br, I); (2) strong σ complexes in which the fluoride anion attacks a partially positive aromatic carbon, changing the hybridization of arene-C to sp^3; (3) weak σ complexes, where the anion is located over the periphery of the aromatic ring, which may be formed with less nucleophilic halides; and (4) hydrogen-bonding complexes. On the other hand, as shown in Fig. 1f, triazine can use the nitrogen atom as an electron donor to form various noncovalent complexes with compounds of fluorine (YF). In this work, we consider three types of noncovalent interactions: hydrogen bonding (Y = H), halogen bonding (Y = Cl, Br, I) and pnicogen bonding (Y = PH_2, AsH_2). As mentioned before, F^- always leads to the strong σ complex with electron-deficient arene, and therefore is not considered in the present study. We first investigate the binary complexes (**1** · X^- and **1** · YF), and then the ternary complexes (X^- · **1** · YF) are examined. Furthermore, we discuss the various energies to characterize the interplay between **1**-X^- and **1**-YF, and compare the geometric details for some selected complexes.

Computational details

All the geometries were fully optimized at the MP2/aug-cc-pVDZ (aug-cc-pVDZPP for iodine) level of theory using the Gaussian 03 programs [52]. The vibrational frequencies were computed to verify that these optimized structures are indeed minima. Single-point energies were recalculated using aug-cc-pVTZ (aug-cc-pVTZPP for iodine) basis set to obtain more accurate energies. Basis set superposition error (BSSE) correction was carried out following the counterpoise (CP) method [53]. The natural bond orbital (NBO) method [54] has been performed to obtain natural population analysis (NPA) charges for analyzing charge transfer from the anion to arene using the procedures contained within Gaussian 03. The

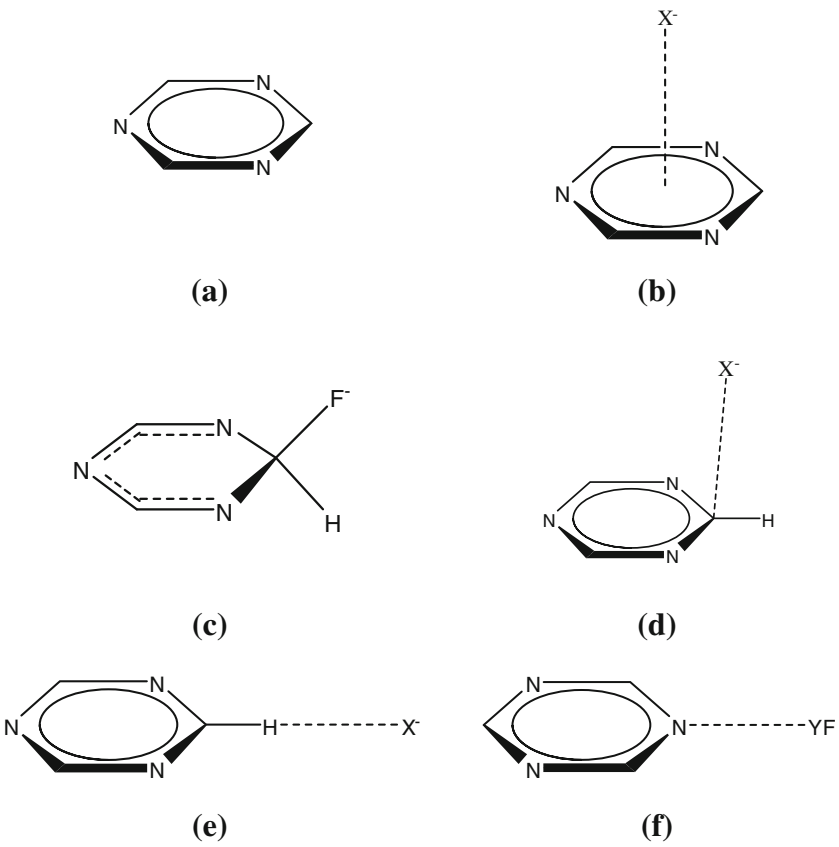

Fig. 1 Receptor (triazine) and binary complexes

Table 1 Equilibrium distance (R, in Å), electron density (ρ, in au), dihedral (D, in °), charge transfer from the anion to the arene (q, in e), and binding energy at the MP2/aug-cc-pVTZ level with BSSE correction (E, in kcal mol^{-1}) for binary complexes

Complex	Binding mode	$R_{1\cdots X^-}$	$\rho_{1\cdots X^-}$	D_{HCNN}	$R_{N\cdots Y}$	$\rho_{N\cdots Y}$	q_{CT}	ΔE
2 (1+**Cl**$^-$)	anion-π	3.146	0.00620				0.0069	−7.79
3 (1+**Cl**$^-$)	σ-type	2.901	0.0157	175.0			0.0429	−8.02
4 (1+**Cl**$^-$)	H-bond	2.301	0.0205				0.0354	−9.70
5 (1+**Br**$^-$)	anion-π	3.312	0.00578				0.0063	−6.99
6 (1+**Br**$^-$)	σ-type	3.095	0.0133	175.8			0.0349	−6.87
7 (1+**Br**$^-$)	H-bond	2.477	0.0177				0.0324	−8.22
8 (1+**I**$^-$)	anion-π	3.557	0.00515				0.0051	−6.04
9 (1+**I**$^-$)	H-bond	2.690	0.0155				0.0309	−6.55
10 (1+HF)					1.722	0.0434		−9.34
11 (1+ClF)					2.248	0.0547		−9.60
12 (1+BrF)					2.280	0.0577		−13.36
13 (1+IF)					2.419	0.0504		−15.82
14 (1+PH_2F)					2.585	0.0264		−6.44
15 (1+AsH_2F)					2.569	0.0295		−7.27

electron densities of complexes have been examined employing atoms in molecules (AIM) analysis [55] with the AIM 2000 program [56].

Results and discussion

Binary complexes

The representative geometric parameters and binding energies of binary complexes are gathered in Table 1, and the values of charge transfer (q_{CT}) from the anion to arene are also listed. Moreover, the electron densities at the corresponding bond and cage critical points are also summarized in Table 1. The cage critical points characterize the anion-π complexes, and the bond critical points characterize the other complexes.

Triazine halide complexes have been extensively investigated by theoretical computation for F^-, Cl^- and Br^- [8]. In this study, three minima have been located for Cl^- and Br^-, but only two minima can be located for I^-. The binding strength is in the sequence of $Cl^- > Br^- > I^-$, and the hydrogen-bonding complex

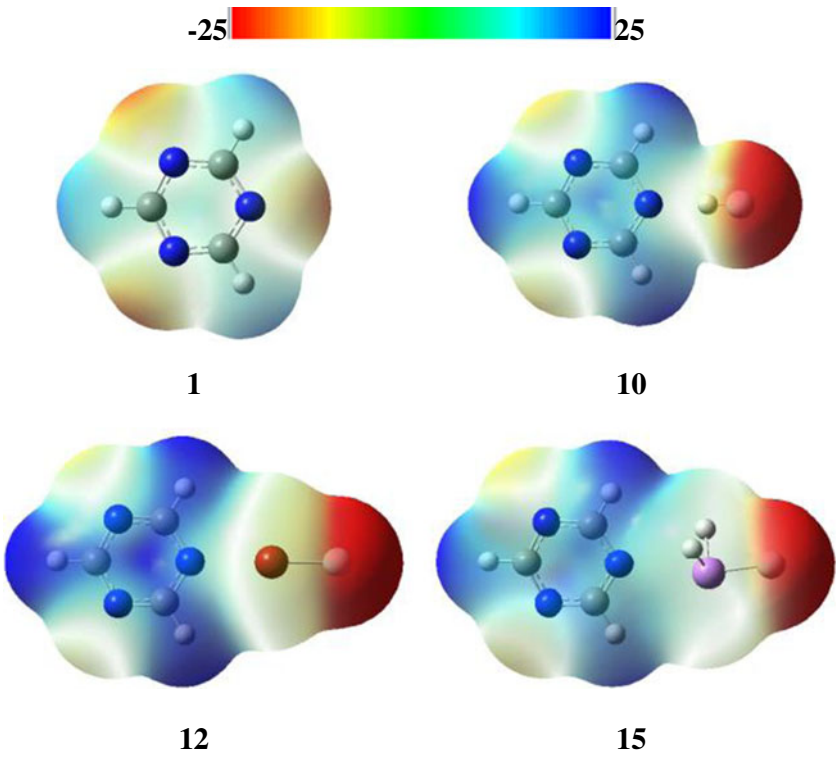

Fig. 2 Electrostatic potential surfaces (ranging from –25 to 25 kcal mol^{-1}) of triazine and selected binary complexes

is the global minimum for all three halides. The present results are consistent with the prior theoretical study for Cl^- and Br^-. The σ complex is more stable than anion-π complex for Cl^-, whereas the anion-π complex is more stable than σ complex for Br^-. This difference implies that Cl^- is a stronger nucleophile than Br^- in the gas phase. At first glance, it seems surprising that the σ-type minimum cannot be located for I^-. But this result is still reasonable, considering that I^- is a rather weak nucleophile in the gas phase. It can be observed that the charge transfer (q_{CT}) values in anion-π complexes are obviously smaller than those in σ-type and hydrogen-bonding complexes.

The molecular electrostatic potential (MEP) surfaces of triazine and three representative complexes are illustrated in Fig. 2. The MEP map of triazine elucidates its dual behavior. An area of positive surface concentrates on the center of ring and expands to the hydrogen atoms along the C-H bonds, which provides various bingding sites for anions. On the other hand, the negative charge is distributed around the nitrogen atoms, which can be used as an electron donor to form noncovalent complexes with compounds of fluorine. As shown in Fig. 2, these noncovalently electron-withdrawing interactions significantly enhance the area of positive surface in triazine moiety, implying that the anion-arene interactions will become stronger in ternary complexes than in binary complexes. In addition, it can be observed from MEP maps of three complexes that the halogen-bonding interaction (**12**) can induce a more strongly electron-withdrawing effect than hydrogen-bonding (**10**) and pnicogen-bonding (**15**) interactions, which is consistent with the results of binding energies: halogen bonding > hydrogen bonding > pnicogen bonding. As discussed below, in contrast with hydrogen and pnicogen bonding, the halogen bonding indeed results in an unexpected binding behavior for σ complexes.

Ternary complexes

As displayed in Fig. 3, five binding modes are possible to exist for ternary systems, and the calculated results for ternary complexes are gathered in Tables 2, 3, and 4. In contrast with

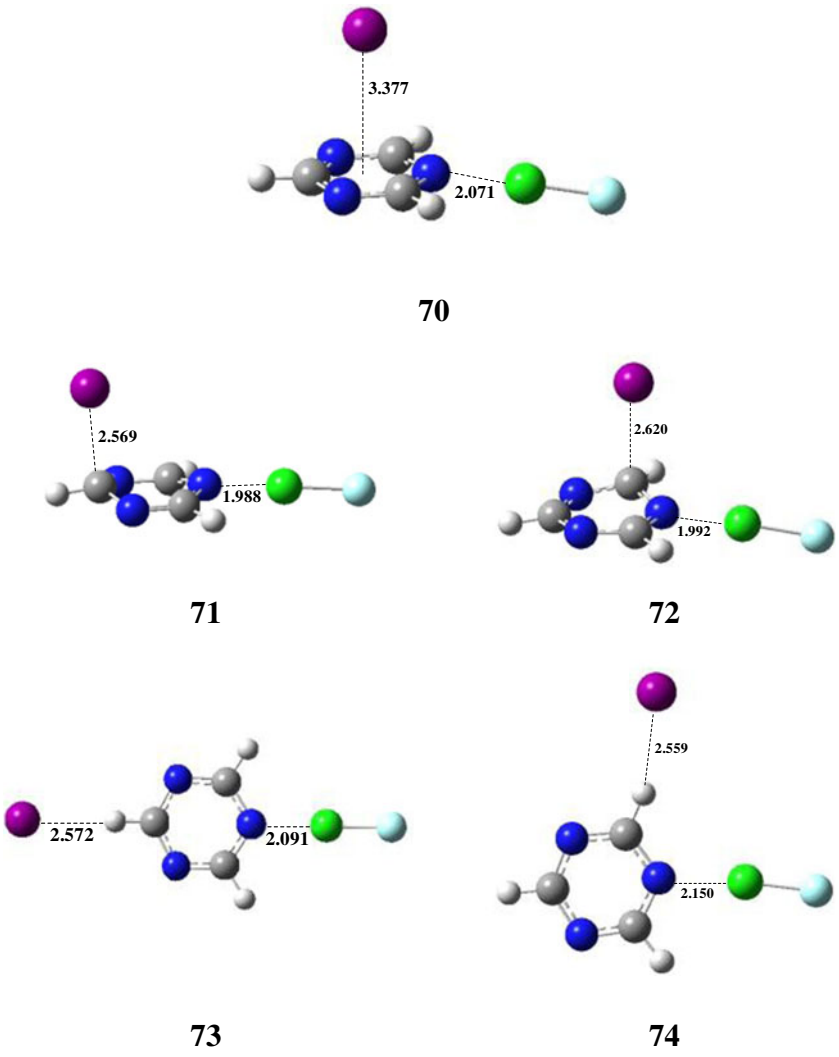

Fig. 3 Five binding modes for I⁻ · 1 · ClF; distances are in Å

Table 2 Equilibrium distance (R, in Å), electron density (ρ, in au), dihedral (D, in °), charge transfer from the anion to the arene (q, in e), and energy data at the MP2/aug-cc-pVTZ level with BSSE correction (E, in kcal mol^{-1}) for Cl$^-$ · 1 · YF complexes

Complex	Binding mode	$R_{1\cdots X^-}$	$\rho_{1\cdots X^-}$	D_{HCNN}	$R_{N\cdots Y}$	$\rho_{N\cdots Y}$	q_{CT}	ΔE	E_{syn}	E_{coop}	E'_{coop}	$\Delta E(X^-\cdot YF)$
16 (1+**Cl**+HF)	anion-π	3.053	0.00716		1.635	0.0555	0.0103	−23.78	−6.64	−1.08	−3.86	−5.56
17 (1+**Cl**+HF)	para-σ-type	2.714	0.0230	170.0	1.607	0.0600	0.0829	−24.39	−7.03	−3.10	−5.07	−3.93
18 (1+**Cl**+HF)	ortho-σ-type	2.722	0.0227	170.5	1.629	0.0562	0.0796	−24.24	−6.88	−0.57	−3.73	−6.31
19 (1+**Cl**+HF)	para-H-bond	2.232	0.0237		1.639	0.0549	0.0446	−24.36	−5.32	−3.21	−4.27	−2.11
20 (1+**Cl**+HF)	ortho-H-bond	2.208	0.0250		1.703	0.0460	0.0485	−23.68	−4.64	−0.15	−2.40	−4.49
21 (1+**Cl**+ClF)	para-σ-type	1.990	0.117	133.4	1.959	0.118	0.6363	−31.98	−14.36	−9.99	−12.18	−4.37
22 (1+**Cl**+ClF)	ortho-σ-type	2.040	0.105	134.9	1.959	0.117	0.5836	−31.32	−13.69	−5.62	−9.66	−8.07
23 (1+**Cl**+ClF)	para-H-bond	2.177	0.0266		2.076	0.0850	0.0533	−27.59	−8.28	−6.70	−7.49	−1.58
24 (1+**Cl**+ClF)	ortho-H-bond	2.144	0.02807		2.129	0.0743	0.0609	−25.11	−5.81	−2.85	−4.33	−2.96
25 (1+**Cl**+BrF)	para-σ-type	2.001	0.114	134.0	2.083	0.0954	0.6223	−36.64	−15.25	−9.99	−12.62	−5.26
26 (1+**Cl**+BrF)	ortho-σ-type	2.045	0.104	135.3	2.084	0.0945	0.5751	−36.11	−14.72	−5.01	−9.87	−9.71
27 (1+**Cl**+BrF)	para-H-bond	2.172	0.0269		2.176	0.0747	0.0543	−32.24	−9.17	−7.18	−8.18	−1.99
28 (1+**Cl**+BrF)	ortho-H-bond	2.131	0.0295		2.214	0.0682	0.0637	−29.87	−6.80	−2.84	−4.82	−3.96
29 (1+**Cl**+IF)	para-σ-type	2.002	0.114	134.1	2.258	0.0739	0.6203	−40.00	−16.16	−9.70	−12.93	−6.46
30 (1+**Cl**+IF)	ortho-σ-type	2.053	0.102	135.9	2.260	0.0731	0.5650	−39.59	−15.75	−3.76	−9.76	−11.99
31 (1+**Cl**+IF)	para-H-bond	2.168	0.0271		2.340	0.0607	0.0551	−35.29	−9.77	−7.25	−8.51	−2.52
32 (1+**Cl**+IF)	ortho-H-bond	2.118	0.0304		2.376	0.0561	0.0665	−33.34	−7.82	−2.20	−5.01	−5.62
33 (1+**Cl**+PH_2F)	para-σ-type	2.678	0.0248	168.7	2.313	0.0464	0.0925	−21.31	−6.85	−2.78	−4.82	−4.07
34 (1+**Cl**+PH_2F)	ortho-σ-type	2.736	0.0221	171.7	2.360	0.0413	0.0808	−23.38	−8.93	0.98	−3.98	−9.91
35 (1+**Cl**+PH_2F)	para-H-bond	2.225	0.0240		2.392	0.0394	0.0454	−20.81	−4.67	−2.91	−3.79	−1.76
36 (1+**Cl**+PH_2F)	ortho-H-bond	2.243	0.0236		2.546	0.0283	0.0571	−23.04	−6.90	2.67	−2.12	−9.57
37 (1+**Cl**+AsH_2F)	para-σ-type	2.619	0.0281	166.5	2.352	0.0465	0.1138	−23.64	−8.36	−3.47	−5.92	−4.89
38 (1+**Cl**+AsH_2F)	ortho-σ-type	2.674	0.0251	169.4	2.375	0.0437	0.0970	−25.49	−10.21	0.40	−4.91	−10.61
39 (1+**Cl**+AsH_2F)	para-H-bond	2.212	0.0247		2.419	0.0404	0.0475	−22.77	−5.80	−3.55	−4.68	−2.25
40 (1+**Cl**+AsH_2F)	ortho-H-bond	2.223	0.0245		2.535	0.0314	0.0613	−24.75	−7.78	2.57	−2.61	−10.35

binary complexes, the noncovalent interactions are much more complicated in ternary complexes. We first examine these interactions and discuss their relation. There are three noncovalent interactions in ternary complexes: **1**-X$^-$, **1**-YF, and X$^-$-YF. The interplay between **1**-X$^-$ and **1**-YF should lead to a cooperative effect, because the direction of charge transfer is synergistic: X$^-$ → **1** → YF. In contrast, the interplay between X$^-$-YF and **1**-YF should lead to a competitive effect, because the direction of charge transfer is antagonistic: X$^-$ → YF ← **1**. The primary purpose of this study is to explore the electron-withdrawing effects of interaction **1**-YF on interaction **1**-X$^-$, and therefore the interplay between **1**-X$^-$ and **1**-YF is our main concern.

We first introduce two energies, the synergetic and cooperative energies, to characterize the interplay between **1**-X$^-$ and **1**-YF. These energies have been successfully used in the studies of similar systems in which various different interactions coexist [33, 37, 51]. The synergetic and cooperative energies can be used as an approximate estimation of energetic stabilization or destabilization obtained in multi-component complexes as a consequence of the coexistence of various interactions. The synergetic energy is computed according to Eq. (1):

$$E_{syn} = \Delta E(X^-\cdot\mathbf{1}\cdot YF) - \Delta E(\mathbf{1}\cdot X^-) - \Delta E(\mathbf{1}\cdot YF) \quad (1)$$

where $\Delta E(X^- \cdot \mathbf{1} \cdot YF)$ are the binding energies of optimized ternary complexes, as listed in Tables 2, 3 and 4, whereas $\Delta E(\mathbf{1} \cdot X^-)$ and $\Delta E(\mathbf{1} \cdot YF)$ are the corresponding binding energies of optimized binary complexes, as listed in Table 1. It should be noted that since the binary σ-type minimum cannot be located for I$^-$, the anion-π binding energy is used as a substitute for σ-type binding energy for I$^-$.

The synergetic energy does not take into account the additional contribution from interaction X$^-$-YF. This problem can be partially solved by adding an additional term that accounts for X$^-$-YF, and the cooperative energy is computed according to Eq. (2):

$$E_{coop} = \Delta E(X^-\cdot\mathbf{1}\cdot YF) - \Delta E(\mathbf{1}\cdot X^-) - \Delta E(\mathbf{1}\cdot YF) - \Delta E(X^-\cdot YF) \quad (2)$$

where $\Delta E(X^- \cdot YF)$ are the interaction energies of X$^-$ with YF, which are calculated by using the corresponding coordinates

Table 3 Equilibrium distance (R, in Å), electron density (ρ, in au), dihedral (D, in °), charge transfer from the anion to the arene (q, in e), and energy data at the MP2/aug-cc-pVTZ level with BSSE correction (E, in kcal mol^{-1}) for $Br^- \cdot 1 \cdot YF$ complexes

Complex	Binding mode	$R_{1\cdots X^-}$	$\rho_{1\cdots X^-}$	D_{HCNN}	$R_{N\cdots Y}$	$\rho_{N\cdots Y}$	q_{CT}	ΔE	E_{syn}	E_{coop}	E'_{coop}	$\Delta E(X^-\cdot YF)$
41 (1+**Br**$^-$+HF)	anion-π	3.219	0.00666		1.641	0.0544	0.0096	−22.47	−6.14	−0.94	−3.54	−5.20
42 (1+**Br**$^-$+HF)	para-σ-type	2.928	0.0185	172.1	1.618	0.0581	0.0653	−22.58	−6.36	−2.58	−4.47	−3.78
43 (1+**Br**$^-$+HF)	ortho-σ-type	2.936	0.0183	172.6	1.64	0.0545	0.0621	−22.38	−6.17	−0.33	−3.25	−5.84
44 (1+**Br**$^-$+HF)	para-H-bond	2.409	0.0202		1.644	0.0540	0.0408	−22.52	−4.96	−2.95	−3.96	−2.01
45 (1+**Br**$^-$+HF)	ortho-H-bond	2.387	0.0211		1.709	0.0452	0.0442	−21.71	−4.15	0.00	−2.08	−4.15
46 (1+**Br**$^-$+ClF)	para-σ-type	2.257	0.0790	140.0	1.974	0.113	0.5237	−26.70	−10.23	−6.18	−8.21	−4.05
47 (1+**Br**$^-$+ClF)	ortho-σ-type	2.325	0.0682	142.5	1.977	0.110	0.4485	−26.41	−9.94	−2.80	−6.37	−7.14
48 (1+**Br**$^-$+ClF)	para-H-bond	2.358	0.0223		2.083	0.0834	0.0484	−25.46	−7.64	−6.14	−6.89	−1.50
49 (1+**Br**$^-$+ClF)	ortho-H-bond	2.335	0.0235		2.139	0.0723	0.0538	−22.87	−5.04	−2.36	−3.70	−2.68
50 (1+**Br**$^-$+BrF)	para-σ-type	2.277	0.0754	141.1	2.096	0.0918	0.4984	−31.49	−11.25	−6.38	−8.82	−4.87
51 (1+**Br**$^-$+BrF)	ortho-σ-type	2.367	0.0620	145.1	2.101	0.0898	0.4013	−31.40	−11.17	−2.59	−6.88	−8.58
52 (1+**Br**$^-$+BrF)	para-H-bond	2.353	0.0226		2.181	0.0738	0.0494	−30.08	−8.50	−6.60	−7.55	−1.90
53 (1+**Br**$^-$+BrF)	ortho-H-bond	2.323	0.0242		2.22	0.0671	0.0565	−27.57	−5.99	−2.39	−4.19	−3.60
54 (1+**Br**$^-$+HF)	para-σ-type	2.273	0.0761	140.9	2.271	0.0716	0.5025	−34.86	−12.17	−6.13	−9.15	−6.04
55 (1+**Br**$^-$+HF)	ortho-σ-type	2.368	0.0618	145.3	2.276	0.0701	0.3989	−34.97	−12.28	−1.52	−6.90	−10.76
56 (1+**Br**$^-$+HF)	para-H-bond	2.349	0.0227		2.344	0.0601	0.0501	−33.12	−9.08	−6.68	−7.88	−2.40
57 (1+**Br**$^-$+HF)	ortho-H-bond	2.307	0.0249		2.38	0.0555	0.0596	−30.97	−6.93	−1.83	−4.38	−5.10
58 (1+**Br**$^-$+PH_2F)	ortho-σ-type	2.937	0.0183	173.4	2.381	0.0395	0.0689	−21.46	−8.15	0.95	−3.60	−9.10
59 (1+**Br**$^-$+PH_2F)	para-H-bond	2.404	0.0203		2.403	0.0386	0.0414	−18.97	−4.31	−2.63	−3.47	−1.68
60 (1+**Br**$^-$+PH_2F)	ortho-H-bond	2.411	0.0204		2.557	0.0278	0.0543	−20.84	−6.18	2.30	−1.94	−8.48
61 (1+**Br**$^-$+AsH_2F)	para-σ-type	2.885	0.0203	170.7	2.374	0.0443	0.0746	−21.66	−7.52	−2.68	−5.10	−4.84
62 (1+**Br**$^-$+AsH_2F)	ortho-σ-type	2.889	0.0201	171.9	2.395	0.0418	0.0792	−23.49	−9.35	0.54	−4.41	−9.89
63 (1+**Br**$^-$+AsH_2F)	para-H-bond	2.391	0.0209		2.427	0.0397	0.0433	−20.87	−5.38	−3.23	−4.31	−2.15
64 (1+**Br**$^-$+AsH_2F)	ortho-H-bond	2.389	0.0213		2.544	0.0308	0.0591	−22.45	−6.97	2.19	−2.39	−9.16

frozen in the geometries of the ternary complexes. $\Delta E(X^- \cdot YF)$ are also listed in Tables 2, 3, and 4. The values of $\Delta E(X^- \cdot YF)$ in ortho-position complexes are obviously more negative than those in para-position complexes, because the distances between X^- and YF in ortho-position complexes are much smaller than those in para-position complexes.

Although E_{coop} is an improvement on E_{syn}, E_{coop} still has a problem. As discussed below, in some cases, a positive E_{coop} does not mean that there is no cooperative effect between **1**-X^- and **1**-YF. In Eq. (2), we use the interaction energy of isolated $X^- \cdot YF$ binary system because we cannot isolate the contribution of X^--YF interaction from the whole ternary system. But as mentioned before, there is a competitive effect between X^--YF and **1**-YF in ternary system because the direction of charge transfer is antagonistic. A typical example is the comparison between complexes **35** and **36**. A stronger X^--YF interaction in **36** (−9.57 kcal mol^{-1}) than in **35** (−1.76 kcal mol^{-1}), indeed results in a larger **1**-YF distance in **36** (2.546 Å) than in **35** (2.392 Å). This competitive effect also exists to a lesser extent in other complexes. The molecular characteristics, such as MEP surface and charge distribution, in ternary systems are different from those in isolated binary systems. Therefore, the isolated X^--YF interaction energy overestimates its contribution to the binding energy of the whole ternary system. The truly energetic characterization of cooperative effect between **1**-X^- and **1**-YF should be the value between E_{syn} and E_{coop}. Herein we simply suggest E'_{coop}, the mean value of E_{syn} and E_{coop}, as a more appropriately energetic characterization of cooperativity between **1**-X^- and **1**-YF, as computed according to Eq. (3):

$$E'_{coop} = \left(E_{syn} + E_{coop}\right)/2 \quad (3)$$

We give some specific examples to explain why E'_{coop} is more appropriate than E_{syn} and E_{coop} for describing the cooperativity between **1**-X^- and **1**-YF. As shown in Table 2, E_{syn}, E_{coop} and E'_{coop} for complex **33** are −6.85, −2.78, and −4.82 kcal mol^{-1}, respectively, whereas these energies for complex **34** are −8.93, 0.98, and −3.98 kcal mol^{-1}, respectively. If we take E_{syn} as the criterion, it seems that the cooperative effect in **34** is stronger than that in **33** because **34** possesses a more negative E_{syn} (−8.93 kcal mol^{-1}) than **33** (−6.85 kcal mol^{-1}), but this is not the case. The equilibrium distances of C-Cl^- (2.678 Å) and N-P (2.313 Å) for **33** are shorter than those

Table 4 Equilibrium distance (R, in Å), electron density (ρ, in au), dihedral (D, in °), charge transfer from the anion to the arene (q, in e), and energy data at the MP2/aug-cc-pVTZ level with BSSE correction (E, in kcal mol^{-1}) for $I^- \cdot 1 \cdot YF$ complexes

Complex	Binding mode	$R_{1\cdots X^-}$	$\rho_{1\cdots X^-}$	D_{HCNN}	$R_{N\cdots Y}$	$\rho_{N\cdots Y}$	q_{CT}	ΔE	E_{syn}	E_{coop}	E'_{coop}	$\Delta E(X^-\cdot YF)$
65 (1+I⁻+HF)	anion-π	3.459	0.00595		1.651	0.0530	0.0082	−20.88	−5.49	−0.73	−3.11	−4.76
66 (1+I⁻+HF)	para-σ-type	3.197	0.0146	173.6	1.630	0.0561	0.0507	−20.64	−5.26	−1.70	−3.48	−3.56
67 (1+I⁻+HF)	ortho-σ-type	3.216	0.0143	174.2	1.651	0.0528	0.0455	−20.42	−5.04	0.23	−2.41	−5.27
68 (1+I⁻+HF)	para-H-bond	2.623	0.0176		1.648	0.0534	0.0390	−20.43	−4.54	−2.63	−3.59	−1.91
69 (1+I⁻+HF)	ortho-H-bond	2.598	0.0185		1.716	0.0444	0.0427	−19.48	−3.59	0.22	−1.69	−3.81
70 (1+I⁻+ClF)	anion-π	3.377	0.00676		2.071	0.0859	0.0124	−24.17	−8.53	−4.40	−6.47	−4.13
71 (1+I⁻+ClF)	para-σ-type	2.560	0.0544	145.3	1.988	0.108	0.4266	−22.54	−6.90	−3.18	−5.04	−3.72
72 (1+I⁻+ClF)	ortho-σ-type	2.620	0.0482	147.5	1.992	0.106	0.3638	−22.44	−6.79	−0.37	−3.58	−6.42
73 (1+I⁻+ClF)	para-H-bond	2.572	0.0194		2.091	0.0817	0.0464	−23.04	−6.89	−5.48	−6.19	−1.41
74 (1+I⁻+ClF)	ortho-H-bond	2.559	0.0200		2.150	0.0702	0.0502	−20.40	−4.25	−1.82	−3.04	−2.43
75 (1+I⁻+BrF)	anion-π	3.377	0.00687		2.169	0.0756	0.0134	−29.02	−9.61	−4.05	−6.83	−5.56
76 (1+I⁻+BrF)	para-σ-type	2.587	0.0512	146.9	2.109	0.0884	0.3943	−27.47	−8.06	−3.58	−5.82	−4.48
77 (1+I⁻+BrF)	ortho-σ-type	2.650	0.0451	149.4	2.112	0.0870	0.3320	−27.56	−8.16	−0.36	−4.26	−7.80
78 (1+I⁻+BrF)	para-H-bond	2.568	0.0195		2.186	0.0729	0.0473	−27.64	−7.73	−5.93	−6.83	−1.80
79 (1+I⁻+BrF)	ortho-H-bond	2.546	0.0205		2.227	0.0660	0.0529	−25.02	−5.11	−1.84	−3.48	−3.27
80 (1+I⁻+IF)	anion-π	3.366	0.00688		2.332	0.0613	0.0156	−32.44	−10.58	−2.99	−6.79	−7.59
81 (1+I⁻+IF)	para-σ-type	2.571	0.0531	146.0	2.281	0.0696	0.4128	−30.77	−8.91	−3.26	−6.09	−5.65
82 (1+I⁻+IF)	ortho-σ-type	2.675	0.0428	151.0	2.287	0.0680	0.3077	−31.29	−9.43	0.38	−4.53	−9.81
83 (1+I⁻+IF)	para-H-bond	2.563	0.0197		2.348	0.0595	0.0481	−30.64	−8.28	−6.00	−7.14	−2.28
84 (1+I⁻+IF)	ortho-H-bond	2.529	0.0212		2.385	0.0548	0.0564	−28.34	−5.97	−1.35	−3.66	−4.62
85 (1+I⁻+PH_2F)	ortho-σ-type	3.185	0.0151	174.3	2.399	0.0381	0.0595	−18.64	−6.16	1.83	−2.17	−7.99
86 (1+I⁻+PH_2F)	para-H-bond	2.617	0.0178		2.414	0.0377	0.0396	−16.88	−3.89	−2.30	−3.10	−1.59
87 (1+I⁻+PH_2F)	ortho-H-bond	2.615	0.0181		2.565	0.0274	0.0529	−18.29	−5.30	1.91	−1.70	−7.21
88 (1+I⁻+AsH_2F)	ortho-σ-type	3.142	0.0164	173.2	2.411	0.0404	0.0671	−21.20	−7.89	0.95	−3.47	−8.84
89 (1+I⁻+AsH_2F)	para-H-bond	2.604	0.0182		2.436	0.0390	0.0415	−18.70	−4.88	−2.84	−3.86	−2.04
90 (1+I⁻+AsH_2F)	ortho-H-bond	2.592	0.0189		2.549	0.0305	0.0577	−19.76	−5.95	1.83	−2.06	−7.78

(2.736 Å and 2.360 Å, respectively) for **34**, indicating that the cooperative effect in **33** should be stronger than that in **34**. This conclusion is also supported by AIM analysis: the values of $\rho_{C\text{-}Cl^-}$ (0.0248 au) and $\rho_{N\text{-}P}$ (0.0464 au) for **33** are larger than those (0.0221 au and 0.0413 au, respectively) for **34**. In fact, a more negative E_{syn} for **34** mainly results from the fact that **34** possesses a more negative $\Delta E(X^- \cdot YF)$ (−9.91 kcal mol^{-1}) than **33** (−4.07 kcal mol^{-1}). If we take E_{coop} as the criterion, it seems that there is no cooperative effect in **34** because **34** possesses a positive E_{coop} (0.98 kcal mol^{-1}), but once again, this is not the case. The equilibrium distances of C-Cl$^-$ (2.736 Å) and N-P (2.360 Å) in **34** are obviously shorter than those in **3** (2.901 Å) and **14** (2.585 Å), respectively, implying that there is a significantly cooperative effect in **34**. AIM analysis gives the same results: the values of $\rho_{C\text{-}Cl^-}$ (0.0221 au) and $\rho_{N\text{-}P}$ (0.0413 au) in **34** are obviously larger than those in **3** (0.0157 au) and **14** (0.0264 au), respectively. In contrast with E_{syn} and E_{coop}, E'_{coop} can solve these two problems simultaneously. **33** possesses a more negative E'_{coop} (−4.82 kcal mol^{-1}) than **34** (−3.98 kcal mol^{-1}), which supports the conclusion that the cooperative effect in **33** is stronger than that in **34**. On the other hand, **34** possesses a negative E'_{coop} (−3.98 kcal mol^{-1}), which is consistent with the fact that there is a significantly cooperative effect in **34**.

E'_{coop} for all ternary complexes have been summarized in Tables 2, 3, and 4. The values of E'_{coop} for halogen-bonding complexes are generally more negative than those for hydrogen-bonding and pnicogen-bonding complexes, implying that halogen-bonding interaction can induce a more strongly electron-withdrawing effect than the other two interactions, which is consistent with the postulation derived from the MEP results.

Some interesting results can be found from Tables 1, 2, 3 and 4. As mentioned before, in binary complexes, both weak σ-type and anion-π complexes can be formed with trazine for Cl$^-$ and Br$^-$, but only anion-π complex can be formed for I$^-$. Moreover, the hydrogen-bonding complex is the global minimum for all three halides in binary complexes. However, in ternary complexes, anion-π complex become unstable and only σ complex can retain in many cases for Cl$^-$ and Br$^-$. Anion-π complex keeps stable only when YF = HF, as shown in Tables 2 and 3. The binding behavior for I$^-$ is different from that for Cl$^-$ and Br$^-$ in two aspects. First, the anion-π complex

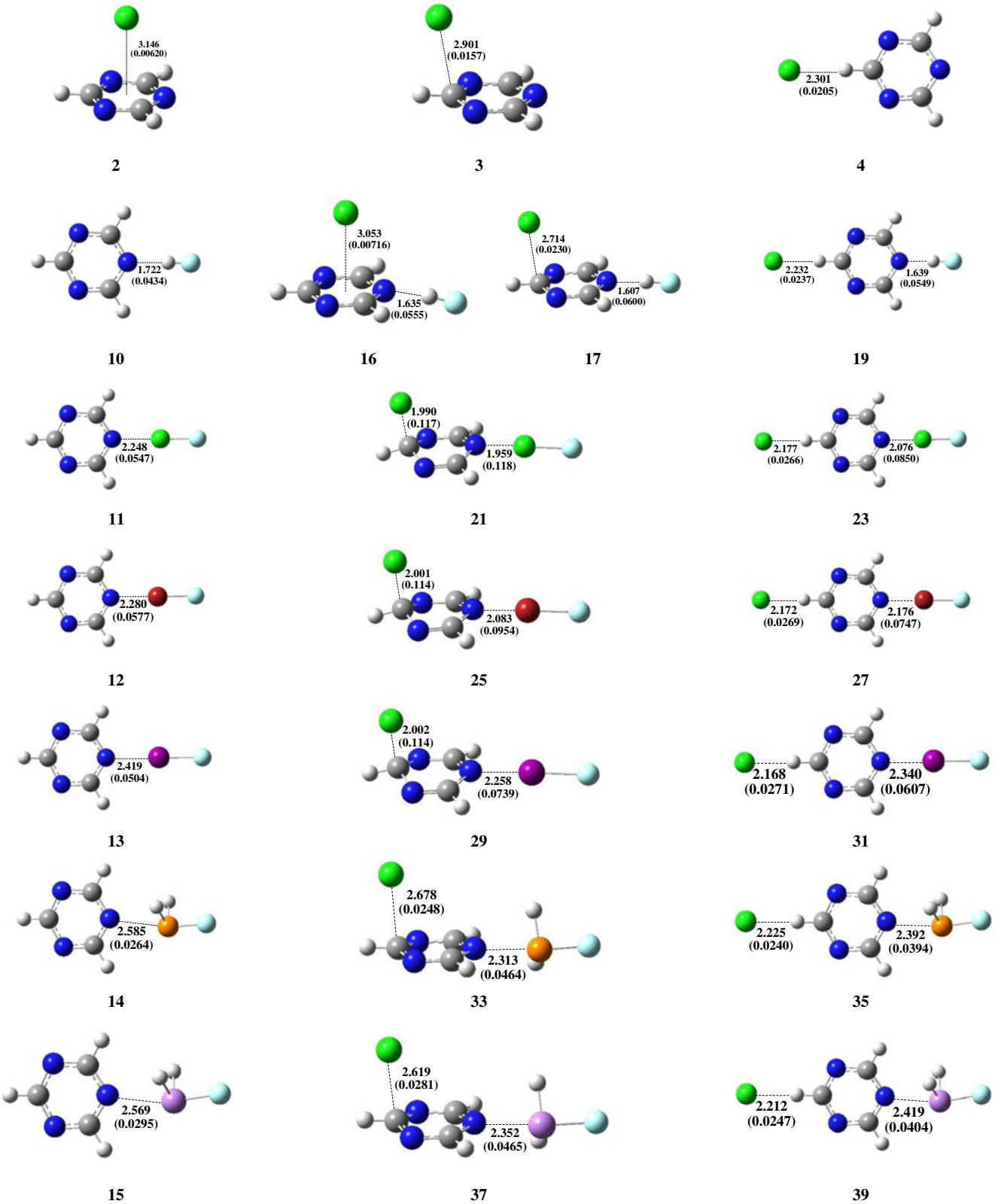

Fig. 4 Optimized geometries of the selected binary and ternary complexes; distances are in Å and electron densities (in parentheses) are in au

for I^- can also keep stable when the noncovalent interaction is halogen bonding, as shown in Table 4. Second, the anion-π complex for I^- is the global minimum when it can retain as a stable structure.

The geometries of anion-π and para-position complexes for $Cl^- \cdot \mathbf{1} \cdot YF$ complexes and the corresponding binary complexes have been illustrated in Fig. 4. The geometries of ortho-position complexes are somewhat different from para-position complexes. For instance, as shown in Fig. 3, the hydrogen bond in complex **73** shows a strictly linear geometry, whereas the hydrogen bond in **74** displays a deviation from the linear geometry because of a strong I^--ClF interaction. It can be observed from Fig. 4 that all the equilibrium distances in ternary complexes are obviously shorter than those in corresponding binary complexes, confirming that there is a significant cooperativity between **1**-X^- and **1**-YF interactions. AIM analysis is consistent with the geometric results: all the electron densities in ternary complexes are larger than those in corresponding binary complexes. In addition, the data gathered in Table 2 indicate an increase in charge transfer from the anion to arene for ternary complexes comparing with corresponding binary complexes.

It can also be observed from Fig. 4 that the values of N-Y distances for π-system bonding (anion-π or σ-type) complexes are generally shorter than those of corresponding hydrogen-bonding complexes, indicating that the π-system bonding structures obtain a more strongly cooperative effect than hydrogen-bonding structures. As discussed below, this difference in cooperative effect has a great influence on the potential energy surfaces around binding sites.

As mentioned before, both MEP surfaces and the values of E'_{coop} imply that halogen-bonding interaction can induce a more strongly electron-withdrawing effect than the other two interactions, which is supported by the geometric results. The hydrogen-bonding distances in complexes **23**, **27** and **31** are shorter than those in complexes **19**, **35** and **39**, indicating that the halogen bonding indeed leads to a more strongly electron-withdrawing effect in these hydrogen-bonding ternary complexes. However, an unexpected result occurs in the σ-type ternary complexes. The C-Cl^- distances in complexes **21**, **25**, and **29** (ranging from 1.990 to 2.002 Å) are much shorter than those in complexes **17**, **33**, and **37** (ranging from 2.619 to 2.714 Å). The values of $\rho_{C\text{-}Cl}$- in **21**, **25**, and **29** (ranging from 0.114 to 0.117 au) are also much larger than those in **17**, **33**, and **37** (ranging from 0.0230 to 0.0281 au). A range of C-Cl^- distances between 1.990 and 2.002 Å implies that the σ-type interactions in these three complexes have relatively strong covalent character, which is supported by the values (ranging from 0.6203 to 0.6363 e) of charge transfer. In fact, Fig. 4 clearly indicates that the corresponding carbon atoms adopt a tetrahedral geometry in **21**, **25**, and **29**. The attacked carbon atom connects with one hydrogen and two nitrogen atoms, and therefore the dihedral D_{HCNN} can be used to describe the extent of deviation from the planar geometry for the carbon. The values of D_{HCNN} for σ-type complexes have been listed in the tables. The values of D_{HCNN} range from 133.4 to 134.1 ° for complexes **21**, **25** and **29**, strongly suggesting that the attacked carbon atom changes to sp^3 hybridization from sp^2, which is the character of strong σ-type interaction. Similar results are also observed for Br^- and I^-.

It is indeed surprising that the halides other than F^- can attack an aromatic carbon connecting with hydrogen, changing the hybridization of arene-C to sp^3, which is totally different from covalently electron-withdrawing effect. The prior theoretical studies indicate that when the halide anions lie above the aromatic ring, Cl^- and Br^- always form the weak σ-type and/or anion-π complexes with arenes, even if in the strongly electron-deficient arenes, such as tetracyanobenzene. The only exception is ref [3], where the authors reported a strong σ-type complex formed by Cl^- with trifluorotriazine, but in which Cl^- attacks the carbon atom connecting with fluorine not with hydrogen.

Conclusions

In this study, we select triazine (**1**) as a dual receptor molecule to understand the noncovalently electron-withdrawing effects on various anion-arene interactions. Triazine can interact with halide anions (X^-) to form anion-π, σ-type, and hydrogen-bonding complexes. On the other hand, triazine can use the nitrogen atom as an electron donor to form various noncovalent complexes with compounds of fluorine (YF). The ternary complexes $X^- \cdot \mathbf{1} \cdot YF$ (X = Cl, Br and I, Y = H, Cl, Br, I, PH_2 and AsH_2) have been carefully investigated by using theoretical methods. The improved cooperative energy E'_{coop} is suggested as a more appropriately energetic characterization of cooperativity between interactions 1-X^- and 1-YF. This work provides new insight into the interplay between noncovalent interactions and anion-arene interactions. Some interesting and unexpected results are obtained.

The calculations indicate that in binary complexes ($\mathbf{1} \cdot X^-$), both weak σ-type and anion-π complexes can be formed for Cl^- and Br^-, but only anion-π complex can be formed for I^-. In addition, the hydrogen-bonding complex is the global minimum for all three halides in binary complexes. However, in ternary complexes, anion-π complex becomes unstable and only σ complex can remain in many cases for Cl^- and Br^-. Anion-π complex keeps stable only when YF = HF. In contrast with binary complexes, σ complex becomes the global minimum for Cl^- and Br^- in ternary complexes. These changes in binding mode and strength are consistent with the results of covalently electron-withdrawing effects. However, in contrast with the covalently electron-withdrawing substituents, Cl^- and Br^- can attack the aromatic carbon atom to form a strong σ complex when the noncovalently electron-withdrawing effect is induced by halogen bonding. The binding behavior for I^- is different from that for Cl^- and Br^- in two aspects. First, the anion-π complex for I^- can also keep stable when the

noncovalent interaction is halogen bonding. Second, the anion-π complex for I^- is the global minimum when it can retain as a stable structure. All the results clearly indicate that the noncovalently electron-withdrawing effects have a great influence on the anion-arene interactions.

Acknowledgments Supported by the High Performance Computing Center, Kunming Institute of Botany, CAS, China.

References

1. Quiñonero D, Garau C, Rotger C, Frontera A, Ballester P, Costa A, Deyà PM (2002) Anion-π interactions: do they exist? Angew Chem, Int Ed 41:3389–3392
2. Schottel BL, Chifotides HT, Dunbar KR (2008) Anion-π interactions. Chem Soc Rev 37:68–83
3. Mascal M, Armstrong A, Bartberger MD (2002) Anion-aromatic bonding: a case for anion recognition by π-acidic rings. J Am Chem Soc 124:6274–6276
4. Alkorta I, Rozas I, Elguero J (2002) Interaction of anions with perfluoro aromatic compounds. J Am Chem Soc 124:8593–8598
5. Dawson RE, Hennig A, Weimann DP, Emery D, Ravikumar V, Montenegro J, Takeuchi T, Gabutti S, Mayor M, Mareda J, Schalley CA, Matile S (2010) Experimental evidence for the functional relevance of anion-π interactions. Nat Chem 2:533–538
6. Ballester P (2013) Experimental quantification of anion-π interactions in solution using neutral host-guest model systems. Acc Chem Res 46:874–884
7. Berryman OB, Bryantsev VS, Stay DP, Johnson DW, Hay BP (2007) Structural criteria for the design of anion receptors: the interaction of halides with electron-deficient arenes. J Am Chem Soc 129:48–58
8. Hay BP, Bryantsev VS (2008) Anion-Arene adducts: C-H hydrogen bonding, anion-π interaction, and carbon bonding motifs. Chem Commun 2417–2428
9. Hay BP, Custelcean R (2009) Anion-π interactions in crystal structures: commonplace or extraordinary? Cryst Growth Des 9:2539–2545
10. Frontera A (2013) Encapsulation of anions: macrocyclic receptors based on metal coordination and anion–π interactions. Coord Chem Rev 257:1716–1727
11. Frontera A, Quiñonero D, Deyà PM (2011) Cation–π and anion–π interactions. WIREs Comput Mol Sci 1:440–459
12. Frontera A, Gamez P, Mascal M, Mooibroek TJ, Reedijk J (2011) Putting anion-π interactions into perspective. Angew Chem, Int Ed 50:9564–9583
13. Estarellas C, Bauza A, Frontera A, Quiñonero D, Deyà PM (2011) On the directionality of anion-π interactions. Phys Chem Chem Phys 13:5696–5702
14. Garau C, Frontera A, Quiñonero D, Ballester P, Costa A, Deyà PM (2004) Cation-π versus anion-π interactions: energetic, charge transfer, and aromatic aspects. J Phys Chem A 108:9423–9427
15. Garau C, Frontera A, Quiñonero D, Ballester P, Costa A, Deyà PM (2005) Approximate additivity of anion-π interactions: an Ab initio study on anion-π, anion-π2 and anion-π3 complexes. J Phys Chem A 109:9341–9345
16. Chen Y-S (2013) Theoretical study of interactions between halogen-substituted s-triazine and halide anions. J Phys Chem A 117:8081–8090
17. Schneider H, Vogelhuber KM, Schinle F, Weber JM (2007) Aromatic molecules in anion recognition: electrostatics versus hydrogen -bonding. J Am Chem Soc 129:13022–13026
18. Garau C, Frontera A, Quiñonero D, Ballester P, Costa A, Deya PM (2003) A topological analysis of the electron density in anion-π interactions. Chem Phys Chem 4:1344–1348
19. Zheng X-Y, Shuai Z-G, Wang D (2013) Anion-binding properties of π-electron deficient cavities in Bis(tetraoxacalix[2]arene[2]triazine): a theoretical study. J Phys Chem A 117:3844–3851
20. Kim D, Lee EC, Kim KS, Tarakeshwar P (2007) Cation-π-anion interaction: a theoretical investigation of the role of induction energies. J Phys Chem A 111:7980–7986
21. Kim DY, Singh NJ, Kim KS (2008) Cyameluric acid as anion-π type receptor for ClO_4^- and NO_3^-: π-stacked and edge-to-face structures. J Chem Theory Comput 4:1401–1407
22. Kim DY, Singh NJ, Lee JW, Kim KS (2008) Solvent-driven structural changes in anion-π complexes. J Chem Theory Comput 4:1162–1169
23. Demeshko S, Dechert S, Meyer F (2004) Anion-π interactions in a carousel copper(II)-triazine complex. J Am Chem Soc 126:4508–4509
24. Rosokha YS, Lindeman SV, Rosokha SV, Kochi JK (2004) Halide recognition through diagnostic"anion-π" interactions: molecular complexes of Cl^-, Br^-, and I^- with olefinic and aromatic π receptors. Angew Chem, Int Ed 43:4650–4652
25. de Hoog P, Gamez P, Mutikainen I, Turpeinen U, Reedijk J (2004) An aromatic anion receptor: anion-π interactions do exist. Angew Chem, Int Ed 43:5815–5817
26. Schottel BL, Bacsa J, Dunbar KR (2005) Anion dependence of Ag(I) reactions with 3,6-Bis(2-Pyridyl)-1,2,4,5-Tetrazine (bptz): isolation of the molecular propeller compound $[Ag_2(bptz)_3][AsF_6]_2$. Chem Commun 46–47
27. Mascal M, Yakovlev I, Nikitin EB, Fettinger JC (2007) Fluoride-selective host based on anion-π interactions, ion pairing, and hydrogen bonding: synthesis and fluoride-ion sandwich complex. Angew Chem, Int Ed 46:8782–8784
28. Wang D-X, Zheng Q-Y, Wang Q-Q, Wang M-X (2008) Halide recognition by tetraoxacalix[2]arene[2]triazine receptors: concurrent noncovalent halide-π and lone-pair-π interactions in host−halide −water ternary complexes. Angew Chem, Int Ed 47:7485–7488
29. Kebarle P, Chowdhury S (1987) Electron affinities and electron-transfer reactions. Chem Rev 87:513–534
30. Alberto ME, Mazzone G, Russo N, Sicilia E (2010) The mutual influence of Non-covalent interactions in π-electron deficient cavities: the case of anion recognition by tetraoxacalix[2]-arene[2]triazine. Chem Commun 46:5894–5896
31. Zuo C-S, Quan J-M, Wu Y-D (2007) Oxa-bicyclocalixarenes: a New cage for anions Via C−H · · · anion hydrogen bonds and anion · · · π interactions. Org Lett 9:4219–4222
32. Wang D-X, Wang Q-Q, Han Y, Wang Y, Huang Z-T, Wang M-X (2010) Versatile anion-π interactions between halides and a conformationally rigid Bis(tetraoxacalix[2]arene[2]triazine) cage and their directing effect on molecular assembly. Chem–Eur J 16:13053–13057
33. Lucas X, Estarellas C, Escudero D, Frontera A, Quinonero D, Deya PM (2009) Very long-range effects: cooperativity between anion-π and hydrogen-bonding interactions. Chem Phys Chem 10:2256–2264
34. Escudero D, Frontera A, Quinonero D, Deya PM (2009) Interplay between anion-π and hydrogen bonding interactions. J Comput Chem 30:75–82
35. Quinonero D, Frontera A, Garau C, Ballester P, Costa A, Deya PM (2006) Interplay between cation–π, anion–π and π–π interactions. Chem Phys Chem 7:2487–2491
36. Frontera A, Quinonero D, Costa A, Ballester P, Deya PM (2007) MP2 Study of cooperative effects between cation–π, anion–π and π–π interactions. New J Chem 31:556–560
37. Estarellas C, Frontera A, Quinonero D, Deya PM (2011) Theoretical study on cooperativity effects between anion–π and halogen-bonding interactions. Chem Phys Chem 12:2742–2750

38. Das A, Choudhury SR, Estarellas C, Dey B, Frontera A, Hemming J, Helliwell M, Gamez P, Mukhopadhyay S (2011) Supramolecular assemblies involving anion–π and lone pair–π interactions: experimental observation and theoretical analysis. Cryst Eng Comm 13: 4519–4527
39. Seth SK, Sarkar D, Kar T (2011) Use of π–π forces to steer the assembly of chromone derivatives into hydrogen bonded supramolecular layers: crystal structures and hirshfeld surface analyses. Cryst Eng Comm 13:4528–4535
40. Seth SK, Saha I, Estarellas C, Frontera A, Kar T, Mukhopadhyay S (2011) Supramolecular self-assembly of M-IDA complexes involving lone-pair · · · π interactions: crystal structures, hirshfeld surface analysis, and DFT calculations [H_2IDA = iminodiacetic acid, M = Cu(II), Ni(II)]. Cryst Growth Des 11:3250–3265
41. Choudhury SR, Gamez P, Robertazzi A, Chen CY, Lee HM, Mukhopadhyay S (2008) Experimental observation of supramolecular Carbonyl-π/π-π/π-carbonyl and Carbonyl-π/π-π/π-anion assemblies supported by theoretical studies. Cryst Growth Des 8: 3773–3784
42. Seth SK, Sarkar D, Jana AD, Kar T, Mukhopadhyay S (2011) On the possibility of tuning molecular edges to direct supramolecular self-assembly in coumarin derivatives through cooperative weak forces: crystallographic and hirshfeld surface analyses. Cryst Growth Des 11:4837–4849
43. Choudhury SR, Dey B, Das S, Gamez P, Robertazzi A, Chan KT, Lee HM, Mukhopadhyay S (2009) Supramolecular lone pair−π/π−π/π−anion assembly in a Mg(II)−malonate−2-aminopyridine−nitrate ternary system. J Phys Chem A 113:1623–1627
44. Das A, Choudhury SR, Dey B, Yalamanchili SK, Helliwell M, Gamez P, Mukhopadhyay S, Estarellas C, Frontera A (2010) Supramolecular assembly of Mg(II) complexes directed by associative lone Pair−π/π−π/π−Anion−π/π−Lone pair interactions. J Phys Chem B 114:4998–5009
45. Li Q-Z, Lin Q-Q, Li W-Z, Cheng J-B, Gong B-A, Sun J-Z (2008) Cooperativity between the halogen bond and the hydrogen bond in $H_3N \cdots XY \cdots HF$ complexes (X, Y=F, Cl, Br). Chem Phys Chem 9: 2265–2269
46. Li Q-Z, Li R, Liu Z-B, Li W-Z, Cheng J-B (2011) Interplay between halogen bond and lithium bond in MCN-LiCN-XCCH (M = H, Li, and Na; X = Cl, Br, and I) complex: the enhancement of halogen bond by a lithium bond. J Comput Chem 32:3296–3303
47. Li Q-Z, Li R, Liu X-F, Li W-Z, Cheng J-B (2012) Concerted interaction between pnicogen and halogen bonds in XCl-FH_2P-NH_3 (X=F, OH, CN, NC, and FCC). Chem Phys Chem 13:1205–1212
48. Alkorta I, Blanco F, Elguero J, Estarellas C, Frontera A, Quinonero D, Deya PM (2009) Simultaneous interaction of tetrafluoroethene with anions and hydrogen-bond donors: a cooperativity study. J Chem Theory Comput 5:1186–1194
49. Alkorta I, Sanchez-Sanz G, Elguero J, Del Bene JE (2012) Influence of hydrogen bonds on the P · · · P pnicogen bond. J Chem Theory Comp 8:2320–2327
50. Janet E, Del Bene JE, Alkorta I, Goar S-S, Elguero J (2013) Phosphorus as a simultaneous electron-pair acceptor in intermolecular P · · · N pnicogen bonds and electron-pair donor to Lewis acids. J Phys Chem A 117:3133–3141
51. Lu Y-X, Liu Y-T, Li H-Y, Zhu X, Liu H-L, Zhu W-L (2012) Energetic effects between halogen bonds and anion-π or lone pair-π interactions: a theoretical study. J Phys Chem A 116:2591–2597
52. Frisch MJ, et al. (2003) Gaussian 03; Gaussian, Inc.: Wallingford, CT
53. Boys SF, Bernardi F (1970) Calculation of small molecular interactions by differences of separate total energies – some procedures with reduced errors. Mol Phys 19:553–566
54. Reed AE, Curtiss LA, Weinhold F (1988) Intermolecular interactions from a natural bond orbital. Donor-acceptor viewpoint. Chem Rev 88:899–926
55. Bader RWF (1990) Atoms in molecules. A quantum theory. Clarendon, Oxford
56. Biegler-König F (2000) AIM2000. University of Applied Sciences, Bielefeld